NASA TECHNICAL TRANSLATION NASA TT F-16349

ANALYSIS OF TERRAIN CONDITIONS IN THE LANDING SITE OF THE MARS-6 AUTOMATIC INTERPLANETARY STATION

R.B.Zezin, V. P. Karyagin, I.P. Mamoshina,
N.A. Morozov, V.M. Pavlova, M.K. Rozhdestvenskiy,
V.G.Fokin

Translation of "Analiz rel'yefnykh usloviy v rayone posadki SA AMS "Mars-6," Kosmicheskiye issledovaniya, Vol. 13, No. 1, January-February, 1975, p. 99-107

NATIONAL AERONAUTICS AND SPACE ADMINISTRATION
WASHINGTON, D.C. 20546 MAY 1975

STANDARD TITLE PAGE

1. Report No.	2. Government Accession No.	3. Recipient's Catalog No.
NASA TT F-16,349		

4. Title and Subtitle	5. Report Date
ANALYSIS OF TERRAIN CONDITIONS IN THE LANDING SITE OF THE MARS-6 AUTOMATIC INTERPLANETARY STATION	May 1975
	6. Performing Organization Code

7. Author(s)	8. Performing Organization Report No.
R.B. Zezin, V.P. Karyagin, I.P. Mamoshina, N.A. Morozov, V.M. Pavlova, M.K. Rozhdestvenskiy, V.G. Fokin	
	10. Work Unit No.

9. Performing Organization Name and Address	11. Contract or Grant No.
Leo Kanner Associates Redwood City, CA 94063	NASw-2481
	13. Type of Report and Period Covered
12. Sponsoring Agency Name and Address	Translation
NATIONAL AERONAUTICS AND SPACE ADMINISTRATION, WASHINGTON, D.C. 20546	14. Sponsoring Agency Code

15. Supplementary Notes

Translation of "Analiz rel'yefnykh usloviy v rayone posadki SA AMS "Mars-6," Kosmicheskiye issledovaniya, Vol. 13, No.1, January-February, 1975, p. 99-107.

16. Abstract On 12 March 1974 the descent module (DM) of the Mars-6 automatic interplanetary station reached the surface of Mars in the designated landing site. The descent of DM -- from atmospheric entry and aerodynamic braking to parachute-assisted descent inclusively -- followed the program. During the parachute descent, lasting approximately 150 sec, direct measurements of the parameters of the Martian atmosphere were made the first time. Based on all available information on the landing site, a detailed analysis was made of the terrain of the DM landing site.

17. Key Words (Selected by Author(s))	18. Distribution Statement
	Unclassified-Unlimited

19. Security Classif. (of this report)	20. Security Classif. (of this page)	21. No. of Pages	22. Price
Unclassified	Unclassified	15	

ANALYSIS OF TERRAIN CONDITIONS IN THE LANDING SITE OF THE MARS-6 AUTOMATIC INTERPLANETARY STATION

R.B. Zezin, V.P. Karyagin, I.P. Mamoshina, N.A. Morozov, V.M. Pavlova, M.K. Rozhdestvenskiy, V.G. Fokin

On 12 March 1974 the descent module (DM) of the Mars-6 /99* Automatic Interplanetary Station (AIS) reached the surface of Mars in the designated landing site. The descent of the DM -- from atmospheric entry and aerodynamic braking to parachute-assisted descent inclusively -- followed the program. During the parachute descent, lasting ≈ 150 sec, direct measurements of the parameters of the Martian atmosphere were made the first time. Based on all available information on the landing site, a detailed analysis was made of the terrain of the DM landing site.

General Characteristics of the Landing Site

The landing site of the Mars-6 DM was selected in accordance with the scientific missions of the flight, with technical requirements in the ballistics and aerodynamics of descent in the Martian atmosphere, and with the capabilities of DM control.

Based on the study of the materials of the most recent ground measurements, data of the Mars-2, Mars-3 and Mariner-6, Mariner-7 and Mariner-9 spacecraft in the lowland region of Mare Erythraeum located in the southern hemisphere of Mars, the Mars-6 DM landing site with coordinates of the sighting point $\phi = -24°$, $\lambda = 25°$ (Fig. 1) was selected.

From the data of processing trajectory measurements, the landing of the DM occurred in the designated area of dispersion with nominal point coordinates $\phi = -23°54'$, $\lambda = 19°25'$ (with

* Numbers in the margin indicate pagination in the foreign text.

nominal entry angle θ_{en} = 12.11°). The area of scatter of the landing point coordinates was approximately ± 6° along the track, and ± 0.1° across the track, with a 3σ probability, and was situated entirely in the calculated area of dispersion for which a detailed analysis was made of the physical conditions of landing.

Atmospheric Pressure at the Surface

The total atmospheric pressure at the mean surface level in the equatorial zone of Mars from data measurements obtained with the IR- [infrared] spectrometer of the Mariner-6 and Mariner-7 spacecraft was P_0 = 5.3 ± 0.3 mbar [1]. From the data of ultraviolet, infrared and radio-occultation experiments on board the Mariner-9, the mean pressure in the equatorial belt of latitudes (±30°) was 4.8 mbar for the equatorial radius 3396.8 km [2].

It can be expected that the total pressure at the mean surface level undergoes seasonal fluctuations with a 20-30% amplitude [3], which are associated with changes in the mass of solid carbon dioxide condensed in the polar caps, that is, the pressure throughout the year evidently fluctuates within the limits 5 ± 1 mbar. The landing time was close to the autumnal equinox. /100 Therefore the mean new-surface pressure was assumed to be 5 mbar.

On a 1:5,000,000 map of Mare Erythraeum (Fig. 1), with a resolution of surface terrain elements of 1-2 km, the 6.1 mbar pressure level was taken as the zero level. From this figure we can see that the calculated area of scattering is at the elevation contour lines 1-3 km with respect to this level. Therefore, the pressure drop in this area was ≈ 0.9 mbar (from 5.6 to 4.7 mbar), with a mean pressure of 5.5 mbar. In the actual landing site the pressure drop and the mean pressure were approximately

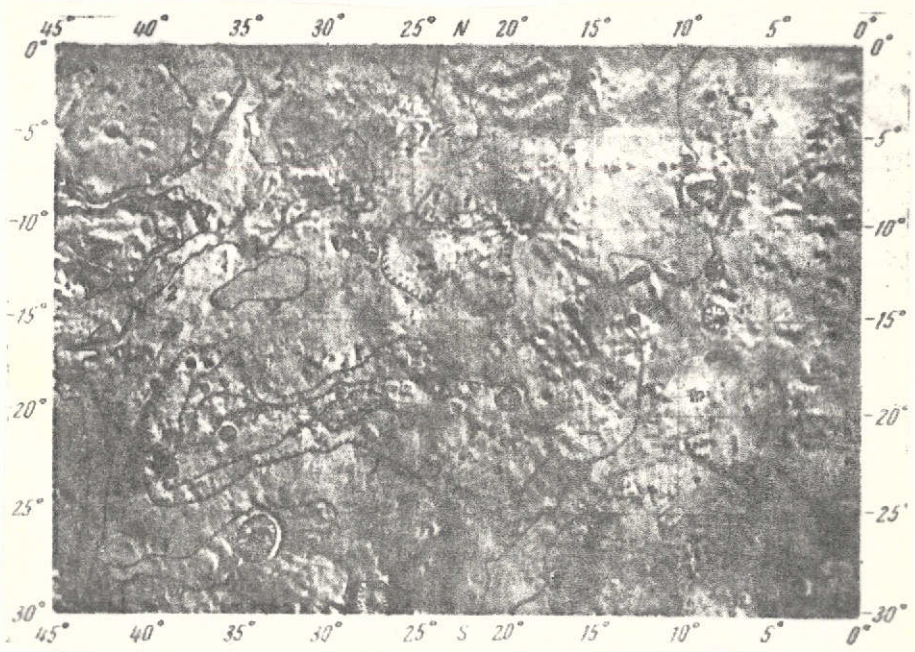

Fig. 1. Map of Mare Erythraeum, 1:5,000,000 scale
Cross. Sighting point; Asterisk. Landing site

the same. In both cases the area with near-surface pressure less than 5 mbar represented ≈ 2% of the area of the calculated scatter of the landing point and the actual area of the scatter of the landing point.

Terrain of Landing Area

The landing area of the Mars-6 DM was situated in the central part of an extensive lowland region of Mare Erythraeum, in turn this being part of the global zone of depression extending in the meridional direction for thousands of kilometers. This zone in the northern hemisphere of Mars includes the following depressions: Mare Acidalium, Chryse Region, and Niliacus Lacus; in the southern hemisphere: Zhemchuzhnyy Zaliv, Pyrrhae Rego, Eos Mare Erythraeum, and Argyre I.

Northwest of the calculated landing site, at a distance of several hundred kilometers is situated the gigantic graben-like

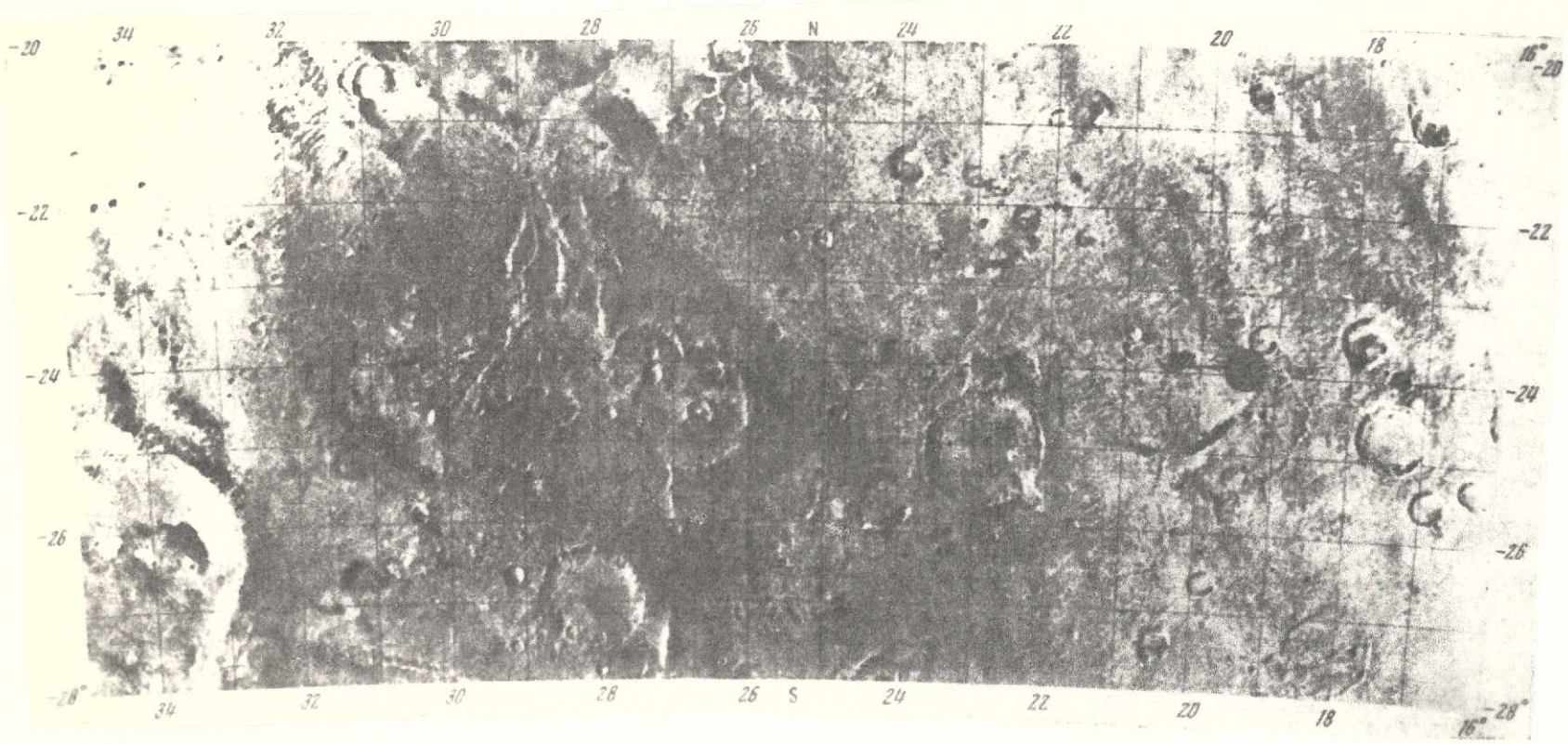

Fig. 2. 1:1,000,000 map of Mare Erythraeum
H.P. Direction of approach and nominal landing site

rift system Coprates [canyon], with whose tectonic activity most probably the elements of the complex chaotic terrain in this area are associated. From analysis of a 1:1,000,000 photomap obtained by Mariner-9 (Fig. 2), a geologo-morphological chart of the landing site of the Mars-6 DM was prepared (Fig. 3). From /103 this chart it follows that in the calculated landing site predominantely two morphological types of terrain are developed: crater and chaotic.

Cratered terrain type. In the landing site of the Mars-6 DM studied, the cratered terrain type occupied most of the area (≈ 75%). The nature of the distribution of craters as well as their morphological features in general outline are similar to the cratered terrain of the lunar surface. Morphologically, the craters of the landing site are subdivided into four main types, listed in order of frequency: 1) flat-bottomed; 2) bowl-shaped; 3) concentric, and 4) craters with a central hummock. In plan form, several craters have irregular, rounded contours; not infrequently craters of polygonal shape are encountered. Most of the craters with diameters greater than 30-40 km are of the flat-bottomed type. With decrease in diameter the number of bowl-shaped craters increases.

In the landing site craters more than 1 km in diameter in all morphological types can be distinctly distinguished by degree of morphological definition in the terrain. They form a continuous morphological series of craters of various degrees of preservation, reflecting the evolution of juvenile forms to the more ancient forms, which from analogy with the lunar surface [4] were conditionally subdivided into three main morphological classes: A, B and C.

Class A includes craters with well-defined swell, distinct crater brow [lip] and with maximum relative depth. Among the

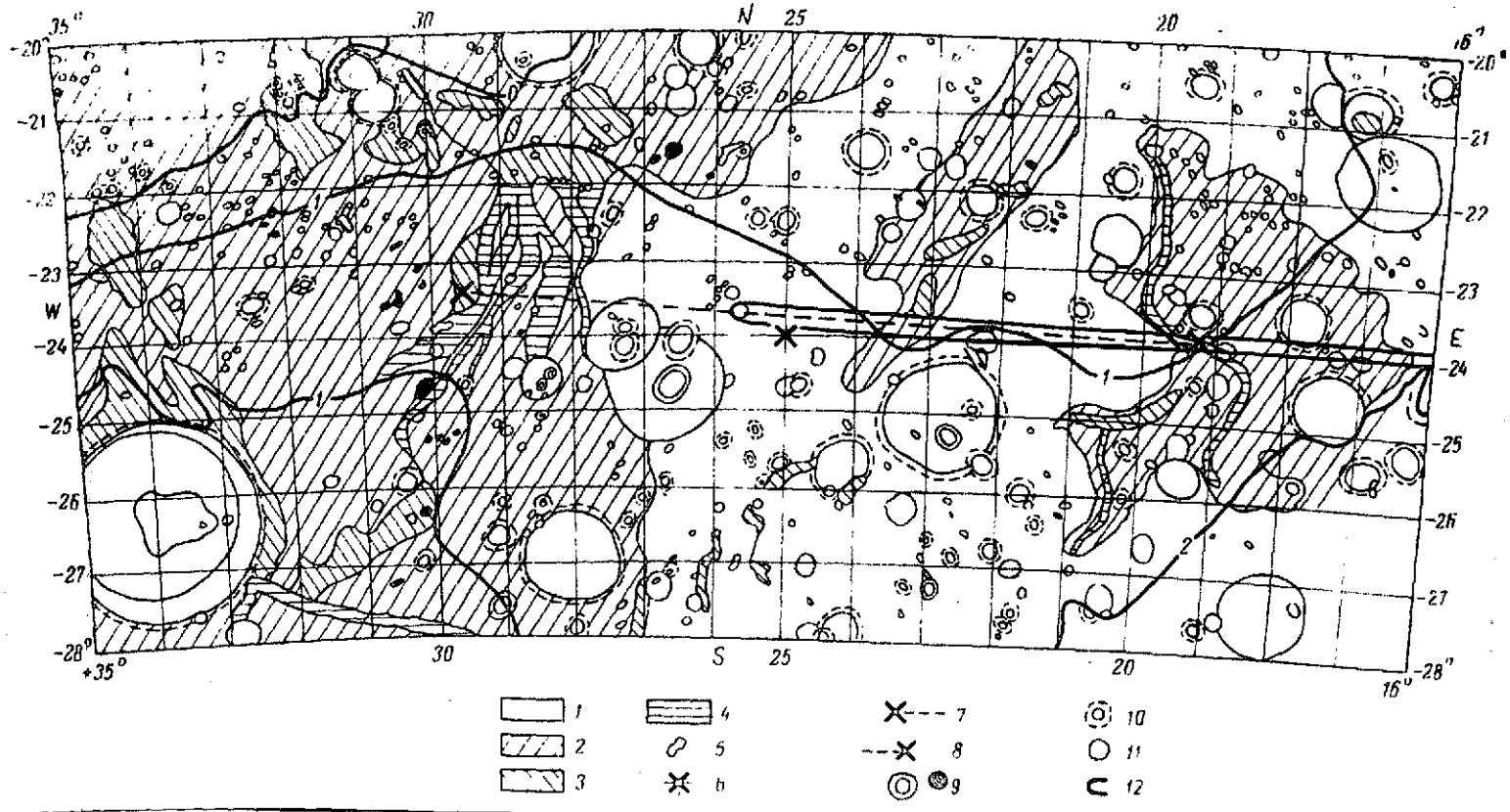

Fig.3. 1:1,000,000 geologo- morphological chart of landing site of DM of Mars-6 AIS.

1. Cratered terrain; 2. Chaotic terrain; 3. Grooves and depressions with detrita; 4. Fissures and valleys; 5. Hills and ridges; 6. Sighting points; 7. Point of atmospheric entry. 8. Landing point. 9. Class A craters; 10. Class B craters. 11. Class C craters; 12. Area of scatter.

craters of this class are encountered the steepest slopes, more than 20-30°. The number of Class A craters does not exceed 2-3% of the total number of craters. In the area of the calculated landing site there were seven Class A craters: 5 with diameter D = 1-5 km, one with D = 8 km, and Alga crater[1] -- with D = 22 km. On analogy with the moon, external zones of ejection of clastic material extending to 4-5 R_{cr} [cr = crater] from crater rim can be associated with Class A craters. The high density of large clastic material within Class A craters, along the swell and in the new-crater zone can present an additional hazard in DM landing.

Class B craters have more rounded forms, weakly defined swell, indistinct rim, and relative depth (D/H) usually greater than 10. Craters in this class are the most widespread in the landing site. The number of Class B craters increases from 50-70% with increase in diameter. Included among Class B craters in the calculated landing site is the largest crater, Mar-Ke -- with D ≃ 100 km, as well as the craters Mar-Ke with D ≃ 60 km, Kf with D = 45 km, Mf with D = 30 km, Bohr with D = 28 km and others (see Fig. 2).

Class C craters are represented by flat-bottomed depressions with intensely rounded forms, flattened rim, and the crater swell is absent or poorly discernable in the photographs. Craters in this class are encountered most often among craters with D ≤30-40 km, however in the landing site there were two very large craters of Class C -- Mar-Qe with D = 90 km and Mar-Qf with D = 55 km, which was situated ≃ 60 km west of the sighting point.

In general outline, the frequencies of craters in

---

[1] In the article we use the preliminary names and nomenclature shown in NASA maps.

morphological Classes A, B and C for the landing site relate as 1:20: 10. Fig. 4 shows the integrated distribution density of craters in the landing site $N_{>D}$ as a function of a diameter for craters in different classes (the logarithmic scale). For comparison, included in the figure are the curves of crater distribution density in the lunar highlands (the area of Tsiolkovskiy Crater) and in the Sinus Medii (Mariner-6 data [5]). From these distribution curves it follows that crater density /104
in the area studied is very close to the crater density in the lunar highlands, and approximately five times greater than in the Sinus Medii, which lies more closely to the Coprates system and is characterized by the predominance of chaotic terrain. It is of interest to note the inflection in the plot of the function $N_{>D}$ (D), which just as for the lunar highlands, occurs at the diameter interval 40-50 km. This possibly reflects the common features of crater formation on Mars and on the Moon in the early stage of evolution of the solar system.

Chaotic terrain type. This morphological terrain type includes sections of the surface with broad development of chaotically arranged, form-wise irregular depressions and upheavals up to 50 km in length and from 3-30 km in width, as well as linear depressions -- grooves and sinuous valleys extending several hundred kilometers in length. However, three predominant directions can be discerned in the chaotic arrangement of these morphological structures: 1) near-meridional; 2) northeasterly ($\approx$ 30° from north); and 3) near-latitudinal.

The distribution of craters in the section with chaotic terrain is characterized by a density which on the average is an order of magnitude less than for the crater type of the locale. Craters with diameters to 30 km are included mainly in morphological Classes A and B; larger craters in Classes B and C have irregular contours and often disclose features of tectonic restructuring.

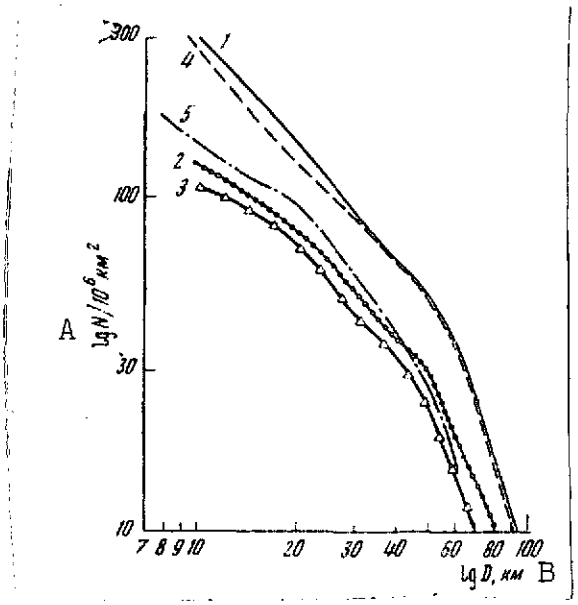

Fig. 4. Distribution of craters in different morphological classes for the landing site of the DM of the Mars-6 AIS (Mare Erythraeum).

1. Craters of all Classes A, B, and C; 2. Craters of Classes A and B; 3. Class C craters. 4. Craters on the lunar highlands; 5. Craters in the area of the initial [illegible] (from Mariner-4 and Mariner-6 data).

Key: A. Lg $N/10^6$, km^2
B. Km

The distribution of slopes in the chaotic terrain locale is close to the distribution of slopes in the lunar highlands. For example, the area occupied by slopes greater than 15° for a base of several meters is about 20%, which is about 4-5 times greater than the area occupied by the analogous slopes in the sections of surface with cratered terrain.

Within the landing site three main surface sections with chaotic terrain type were distinguished.

The first (western) section embraces an extensive territory toward the west and northwest of the calculated landing region and extends further toward the northwest up to rift Coprates [canyon] system. This section lies between two gigantic depressions: toward the south -- Holden crater with D ≈ 150 km, and toward the north, Erythraeum kettle hole with a diameter ≈ 400 km. These depressions are connected with each other by a system of sinuous valleys, which came to be called the ~~Alandon Valleys~~. This system, composed of four main valleys, was taken as the origin for the relatively elevated rimming of

the Holden depression and merges into a single mouth, entering the Erythraeum kettle hole. Sections of the valleys transecting the calculated landing area are from 1-2 km in width (in the upper regions) to 10-30 km (in the lower regions). They have U- and V-shaped transverse profiles with relatively steep slopes.

In several cases there are grounds to assume that the steepness /105
of the valley slopes can exceed 15-20°. Besides the sinuous valleys, typical elements of chaotic terrain are widely developed within this section: depressions of irregular shape and individual hills of isometric contours. Sometimes dark patches can be seen in the depressions, which probably are accumulations of alluvial /106
sandy material, since in several large-scale Mariner-9 photographs, these formations were resolved into characteristic eolian forms of dune and barchan types. Within the western part of the calculated landing area the depressions with dark patches are infrequently seen, however, here there are several rounded hills with diameters 1-20 km.

The second (central) section with chaotic terrain of the locale transects the central part of the calculated landing area in the northeastern direction. This section, in contrast to the western section, is characterized by the accumulation of extensive rounded depressions 10-30 km in size, with numerous dark patches of irregular configuration. As noted above, these patches are probably alluvial sand and dust deposits. These depressions, judging from the morphological definition in the terrain, can be identified as ancient, intensely broken down cratered structures buried by drifts. Within the calculated landing area the accumulations of alluvial material in the form of dunes and barchans evidently occur in the crater Mf (Class B) with D = 30 km and two depressions ≈ 30 km in size.

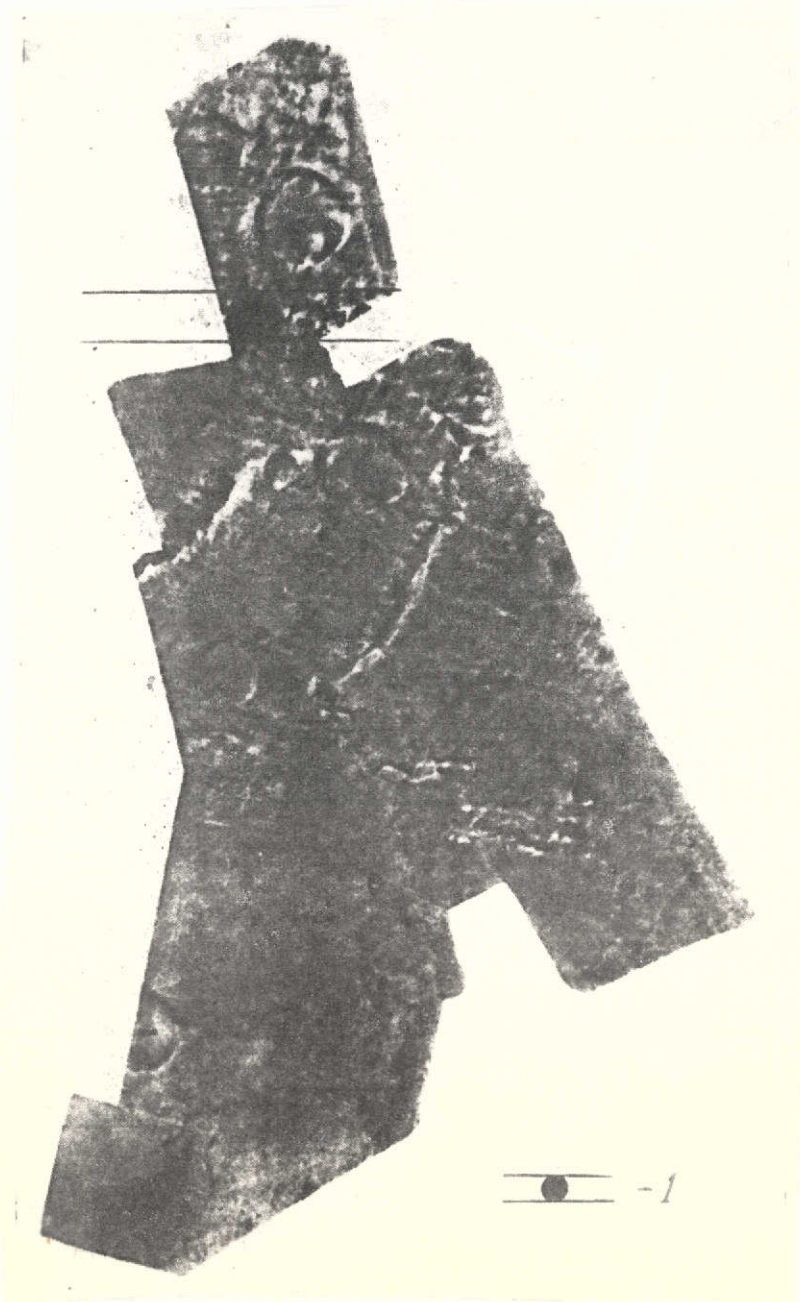

Fig. 5. Fragment of map of landing site of DM of Mars-6 AIS, 1:250,000 scale (area of Samara Valley)

1. Entry corridor and landing site.

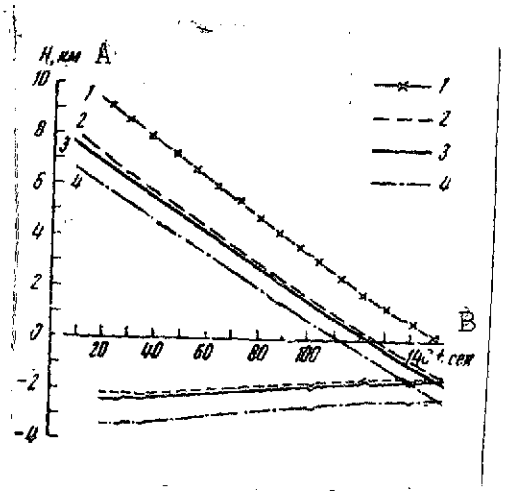

Fig. 6. Profile of terrain of landing site of DM of Mars-6 AIS from data of the analysis of radioaltimeter readings and the calculated descent trajectories.

1. Readings of radioaltimeter during descent of the DM; 2, 3, 4. (Upper). Calculated ballistic descent trajectories for entry angles $\theta = 12 \pm 1.5°$ and given parachute drag $C_x = 1.05$.

2,3,4. (Lower). Reconstruction of profile of terrain corresponding to the calculated descent trajectory and the radioaltimeter readings.

Key: A. H, km
B. 140, t, sec

The third (eastern) section with chaotic terrain type embraces the zone of development of linear formations of the groove and sinuous valley types, which in contrast to Landon Valley, show in the plan form a more complex meandering figure and a multitude of discontinuous tributaries. Within this area three main valleys can be distinguished, with nearly meridional direction: Samara Valley, Sinus Valley and Klota Valley. All three valleys extend into a crater-like depression (Class C) with a 120 km diameter, weakly defined in the terrain. The southern part of this depression can be readily distinguished due to the accumulation of dark, probably, sand-dust material. There are a number of morphological features permitting the assumption that these valleys form a single main system transecting the disintegrated crater indicated. The flattened contours of the valleys within the crater are probably accounted for by erosion of very loose material filling the crater bottom. The central area in the valley system in this section is occupied by Samara Valley. Most of this valley lies within the calculated scatter of the landing site. The extent

of the valley is ≈ 300 km, and its width is 1-12 km. The trend of the valley is predominantly northerly and northeasterly. Morphologically, Samara Valley has much in common with typical terrestrial river valleys. As follows from the large-scale photomap M = 1:250,000 (Fig. 5), in plan form the valley shows a well-defined meandering character with a system of alternating geniculate bends. The sources, situated in the relatively elevated southerly section, are represented by a system of narrow (0.5-1.5 km) branching valleys, combining into a single /107 channel. In the actual landing site, (Fig. 2 and 5) only the sublatitudinal geniculate bend of the valley is included, caused probably by its transecting with a Class B crater, ≈ 15 km in diameter. The extent of this section of the valley is ≈ 60 km, while its width is 3-6 km. Further toward the west, in transecting an ancient crater kettle hole, the valley broadens to 10-12 km, but along this section it can be discerned only with difficulty in the 1:1,000,000 photomap (Fig. 2). The transverse profile of the valley within the landing site is V-shaped in form with a gentle terrace-like scarp in its upper part, whose presence indicates the several stages of valley formation.

Evaluation of the probability of the DM landing in different geologo- morphological sections of the landing site terrain.

Analysis of the DM descent trajectories made it possible to revise the actual area of landing point scatter and the earlier-obtained estimate of the probability of landing in sections with various geologo-morphological situations. For example, the probability of hitting the surface with the cratered terrain type is ≈ 50%, and hitting the surface with chaotic terrain type -- ≈ 50%. The probability of arriving in the largest cratered structures of the scatter area are as follows: 3% -- in the Mf crater with D = 30 km, 1.5% in Dingo-B crater with D = 5 km,

7% -- in a crater with center coordinates $\phi = -24°$, $\lambda = 18.9°$ (D = 15 km), and in Dingo-A crater with D = 20 km -- 4%.

Analysis of the radioaltimeter readings along the section of the parachute-assisted descent and a comparison of the resulting time dependence of change in altitude with the calculated ballistic descent trajectories made it possible to reconstruct the general nature of the terrain profile along the parachute-assisted section down to the landing point extending ≈ 3 km (Fig. 6). Reconstruction of the terrain profile along the DM descent section suggests that the descent and landing of the DM of the Mars-6 AIS occurred in the vicinity of Samara Valley.

REFERENCES

1. Herr, K.C., Horn, D., McAfee, J.M., Pimental, G.C., Astron. J.75, 883 (1970.

2. Conrath, B., Curran, R., Hanel, R. et al., J. Geophys. Res 78, 4267 (1973).

3. Schorn, R.A., Gray, L.D., Astrophys. J. 148, 663 (1967).

4. Florenskiy, K.P., Bagilevskiy, A.T., Gurshtein, et al. in: Sovremennyye predstavleniya o Lune [Modern views on the moon], Moscow, "Nauka" Press, 1972 p. 21.

5. Leighton, R.B., et al., Science 166, 46 (1969).